

FEDSM-ICNMM2010-' 0%)

AN IMMERSED BOUNDARY BASED METHOD FOR STUDYING THERMAL INTERACTION OF PARTICLES IN A VISCOUS FLUID

Zhi-Gang Feng

Department of Mechanical Engineering
University of Texas at San Antonio, Texas
zhigang.feng@gmail.com

Basu D. Paudel

Department of Mechanical and Energy Engineering
University of North Texas, Denton, Texas
BasuPaudel@my.unt.edu

Xing Zhang

Institute of Mechanics, Chinese Academy of Sciences
Beijing, China
zhangx@lm.imech.ac.cn

INTRODUCTION

ABSTRACT

The results of thermal interactions between a solid particle and a fluid have two folds: the motion of fluid affects the heat transfer and energy balance of a particle; and the heat transfer from particles influences the fluid motion. When the temperature of a particle and its surrounding fluid is not the same, heat is transferred between the particle and the fluid. The heat flux influences the properties of the surrounding fluid and changes the dynamics of the sedimentation of the particle. To study the effect of non-isothermal flows to the motion of a particle, we have developed a *Direct Numerical Simulation* (DNS) method that is capable of solving both the momentum equation and heat transfer equation for the computation of thermal interaction between particles and fluid. This numerical method makes use of a finite difference method in combination with the *Immersed Boundary* (IB) method for treating the particulate phase. In particular, the IB concept has been extended to treat thermal boundary condition at the particle surface. A regular Eulerian grid is used to solve the modified momentum and energy equations for the entire flow region simultaneously. In the region that is occupied by the solid particles, a second particle-based Lagrangian grid is used, which tracks particles, and a force density function or an energy density function is introduced to represent the momentum interaction or thermal interaction between particle and fluid. In this paper, the IB based DNS method has been applied to study the fluidization of 12,000 circular particles, the unsteady conduction of a sphere in a stagnant fluid, and the sedimentation of a non-isothermal sphere in a viscous fluid at different Grashof number. Our simulation results show that the sedimentation velocity of the particle depends strongly on the thermal interaction of particle and fluid due to the strong buoyancy force exerted on the particle.

Many of particulate flows that take place in natural and engineering processes involve not only momentum interactions, but also heat or mass transfer between particles and fluids; such examples include the evaporation and combustion of drops, the motion of catalyst particles in chemical reactors, and the fluidization of solid fuels in reacting bed systems. For better understanding the nature of particles and fluid interactions, numerically modeling has increasingly become an efficient and effective tool. In general, there are three common techniques that have been used extensively for the numerical simulations of the particle-fluid momentum interactions: the first approach is *Two-Fluid continuum Model* (TFM), which treats the solid and liquid phases as two fluids governed by separate momentum equations^[1]. The effect of fluid and particle interactions are mainly reflected in the apparent viscosity and the drag coefficient used in the governing equations. The second approach is *Discrete Particle* (or *Element*) *Model* (DPM or DEM)^[2]. This model considers each particle as a point force and determines the position of particles by solving the Lagrangian equation of motion for every particle in the flow field. The force acting on each particle is approximated by an empirical drag force. The third approach, which has gained popularity in the recent years because of the improvement of computational power, is the *Direct Numerical Simulation* (DNS)^[3]. This approach treats the solid particles and the fluid separately. The determination of the solid-fluid interaction is accomplished simultaneously through the solution of the Navier-Stokes equation for the fluid and the equations of motion for particles. In recent years, the *Immersed Boundary* (IB) method based DNS has been showing promising in solving a system of large number particles. The IB method was introduced by Peskin^[4] to account for fluid-solid interactions. The IB based DNS method uses a fixed Cartesian mesh for the

fluid, and a moving, Lagrangian grid for the particle. A force density function is usually defined in conjunction with this method to represent the effect of the particles on the fluid. Various schemes have been proposed to compute the force density functions. Among them, the direct-forcing scheme introduced by Mohd-Yusof^[5] has been a favorite choice because of its simplicity and ease in implementation. IB based DNS has been successfully applied in the study of momentum interaction in particulate flows^[6,7].

Recently IB based DNS has also been employed to study particulate flow with particle-fluid heat interactions^[8,9]. Since many applications of particulate flows involve particles of small size and relatively higher conductivity compared to fluid or gas phase, we can assume particles to be in uniform temperature (Biot number $Bi=0$). In such cases, the Bousinesq assumption can be adopted to account for the variation of fluid density due to temperature gradient.

Two types of grids are used to solve the particle-fluid interactions in the IB based DNS: the first is a fixed Eulerian grid for the entire flow domain and the second is a moving Lagrangian grid for each particle. The modified momentum and energy equations are solved only on the Eulerian grid. The no-slip and the constant temperature boundary conditions on the particle surface and the rigid body motion of particles are enforced only in the Lagrangian grid. To account for the fluid-particle interactions, a force density function and an energy density function are introduced into the momentum and energy equation, respectively. These density functions represent the total effects of the net momentum and energy exchanges between particles and fluid. In this paper, a brief introduction of IB based DNS method is presented; the DNS method is then used to study the fluidization of a large number of circular particles, as well as the sedimentation of non-isothermal spheres in three-dimensional flows.

PROBLEM DESCRIPTION

Combined with direct forcing scheme, the IB based DNS has been implemented successfully to solve particle and fluid momentum interactions by Feng and Michaelides^[6], and Uhlman^[7]. Here, we present a brief description of this method. Consider a particulate flow system composed of circular rigid particles suspended in the two-dimensional incompressible Newtonian fluid, as shown in Figure 1. The entire computational domain, Ω is composed of the fluid region, L , and the solid particle region, $\sum S_i$ ($S_1 + S_2$ in the figure). The domain is surrounded by a boundary, Γ . The boundary or surface of the i -th particle S_i is denoted by ∂S_i .

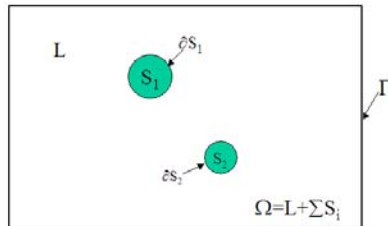


Figure 1: Conceptual model of two circular particles suspended in a fluid.

Based on the concept of IB and the direct-forcing scheme, the fluid field and temperature field for the entire domain Ω , which is occupied by the fluid and the solid particles, can be described by using the following set of dimensionless governing equations:

A. For the velocity field of entire domain:

$$\frac{\partial \vec{u}}{\partial t} + \vec{u} \cdot \nabla \vec{u} = -\nabla p + \frac{1}{Re} \nabla^2 \vec{u} + \frac{Gr}{Re^2} \theta \vec{e}_g + \vec{f}, \quad \vec{x} \in \Omega \quad (1)$$

where \vec{u} , p , and θ are the dimensionless fluid velocity, pressure, and temperature, \vec{f} is the force density accounts the presence of solid boundary in fluid, \vec{e}_g is the unit vector in the direction of gravity, Re is Reynolds number, and Gr is Grashof number.

B. For the force density field:

$$\vec{f} = \frac{\partial \vec{u}}{\partial t} + \vec{u} \cdot \nabla \vec{u} + \nabla p - \frac{1}{Re} \nabla^2 \vec{u} - \frac{Gr}{Re^2} \theta \vec{e}_g \quad \vec{x} \in \sum S_i \quad (2)$$

C. Continuity equation:

$$\nabla \cdot \vec{u} = 0, \quad \vec{x} \in \Omega \quad (3)$$

D. For the velocity field inside a solid particle region:

$$\vec{u} = \vec{U}_i + \vec{\omega}_i \times (\vec{x} - \vec{x}_i) \quad (4)$$

Here, \vec{x}_i is the center of the i -th particle; \vec{U}_i and $\vec{\omega}_i$ are the translational and angular velocities of the particle, respectively.

E. For the motion of the particles:

$$(\rho_r - 1)V_p \frac{d\vec{U}_i}{dt} = \int \vec{f} dV + (\rho_r - 1)V_p \vec{g} + \vec{F}_i^{col} \quad (5)$$

$$\frac{I_p}{\rho_r} (\rho_r - 1) \frac{d\vec{\omega}_i}{dt} = - \int (\vec{x} - \vec{x}_i) \times \vec{f} dV + \vec{T}_i^{col} \quad (6)$$

where ρ_r is the particle-fluid density ratio, V_p and I_p are the volume of a particle and its moment of inertia; \vec{F}_i^{col} and \vec{T}_i^{col} are the resultant force and moment on the i -th particle caused by particle-particle and particle-wall collisions.

F. For the temperature field of entire domain:

$$\frac{\partial \theta}{\partial t} + \vec{u} \cdot \nabla \theta = \frac{1}{Pe} \nabla^2 \theta + q + \lambda, \quad \vec{x} \in \Omega \quad (7)$$

Where θ is temperature field, Pe is fluid Peclet number, q is the heat source or sink, and λ is the energy density function.

G. Energy density function:

$$\lambda = \frac{\partial \theta}{\partial t} + \vec{u} \cdot \nabla \theta - \frac{1}{Pe} \nabla^2 \theta - q, \quad \vec{x} \in \sum S_i \quad (8)$$

H. Uniformity of temperature in the solid region:

$$\theta = \theta_p, \quad \vec{x} \in \sum S_i \quad (9)$$

where θ_p is the particle temperature.

In this paper, the radius of particle is chosen as the characteristic length; the temperature difference between particle and fluid is used as reference temperature, which makes unit temperature for particles and zero temperature for ambient or undisturbed fluid. It must be pointed out that, because of the mass-energy transfer analogy, the governing equations of the equivalent mass transfer problem are identical in form to those of the energy transfer problem. Hence, the numerical scheme that implemented here may be used for the solution of the coupled mass transfer and particle motion problem without any significant modifications.

The above set of equations, together with boundary conditions and initial conditions, is solved numerically using

finite-difference based scheme, as detailed in our previous paper ^[10].

RESULTS AND DISCUSSIONS

Using the IB based DNS method outlined in the previous section, we study three examples of particle and fluid momentum and thermal interactions. The first example is the fluidization of a large number of circular particles by a jet flow. The second example is the unsteady heat conduction of a non-isothermal sphere in a stagnant fluid; results of Nusselt number and temperature fields for this special case are compared with analytical solutions. This example is chosen to serve as a validation of the three-dimensional DNS method for thermal interaction. The last example is the sedimentation of a sphere with different temperatures in a viscous fluid column at different Grashof numbers.

Evolution of a “bubble” in particle-fluid systems

Our first example is to use DNS method to study the momentum interaction between a large number of particles and a viscous fluid. Initially, 12,000 circular particles are closely packed at the bottom of the bed, as shown in the snapshot at $t=0$ in Figure 2; a fluid jet with high velocity is introduced into the bed through its bottom at $t=0$ and it lasts 0.15 s, which creates a “bubble” (a void area of very few particles). The physical parameters used in the simulation are listed in Table 1. Each particle is outlined by 8 grid spaces. To prevent unphysical overlapping between particles or particles and walls, a hybrid collision scheme similar to the one developed by Feng and Michaelides ^[6] is used in the simulations. When the gap between a pair of particles falls below a pre-defined threshold (1 grid space in the present simulation), a repulsive force will be added to the two particles. Figure 2 shows the evolution of the shape and size of a “bubble” as it interacts with surrounding particles. The color is used to identify the initial zones of particles and to provide better visualizations of particle mixing. It is seen that at $t=0.7$, the large “bubble” breaks into two small “bubbles” and eventually collapses.

Such simulation provides a useful tool for studying the hydrodynamics of particulate flows; it can also be used to validate other multiphase models by comparing DNS simulation results with those obtained from TFM or DEM models.

Table 1: Physical parameters used in the DNS simulation of fluidized beds

Solid phase		Liquid phase (water)	
Particle shape	Circular	Fluid viscosity, μ_f	0.01 g/cm s
Number of particles	12000	Fluid density, ρ_f	1.0 g/cm ³
Particle diameter, d	0.2 cm		
Relative density, ρ_r	2.65		
Fluidized bed configuration			
Bed width	16 cm	Orifice width	1 cm
Bed height	48 cm	Jet velocity & pulse duration	800 cm/s, 0.15s.

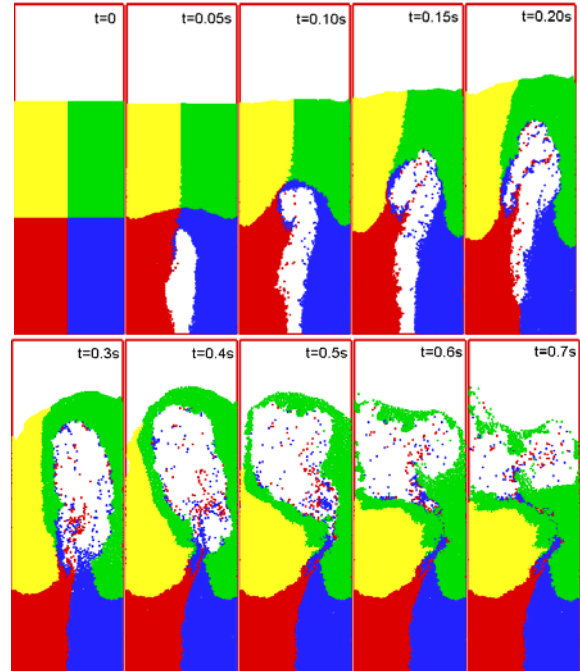


Figure 2: The evolution of a single bubble in a fluidized bed consisting of 12,000 particles. The particles are colored to visualize the mixing.

Unsteady heat conduction from a hot sphere

We consider a special case of a stationary particle immersed in a stagnant fluid at $Gr=0$, in which no buoyancy force exists and fluid remains stationary. Under these conditions, the problem is reduced to a pure conduction problem. For a sphere in a large domain, analytical solutions of unsteady heat conduction from a sphere is readily available and they can be used to validate the numerical results. The temperature field around the sphere follows:

$$\Theta(r, t) = \frac{1}{r} \operatorname{erfc} \left(\frac{r-1}{2\sqrt{t}} \right) \quad (10)$$

where $\operatorname{erfc}(x)$ is complement error function. It can be found that the overall Nusselt number is ^[11]:

$$Nu = 2 \left(1 + \frac{1}{\sqrt{\pi t}} \right) \quad (11)$$

As t approaches infinite, we have $Nu(\infty)=2$ for steady conduction of a sphere. However, the decay, which is in $t^{-1/2}$, is very slow. For example, the time required for $Nu=0.90Nu(\infty)$ is about $t \approx 32$.

For unsteady conduction with $Gr=0$, only the energy equation is needed for obtaining the temperature field. The size of computational domain in this case is chosen to be a $10 \times 10 \times 10$ cube, and the sphere is placed in the center of the cube. The domain size will affect the value of Nusselt number at large time t ; however, the current domain size is sufficient to provide accurate results for short time ($t < 5$). We also tested different grids and time steps. It is found that there is little difference on the Nusselt numbers when a grid of $100 \times 100 \times 100$ is used or a grid of $200 \times 200 \times 200$ is used (time step = 0.001 for both cases), as shown in Figure 3. A smaller time step of 0.0005 is also used, and no noticeable difference is observed. Figure 3 also shows a comparison between the analytical solution and

numerical simulation of overall Nusselt number versus time. Except at beginning ($t < 0.15$) where there is a large impulse based on the theoretical solution of Equation (11), the numerical results agree well with analytical solution.

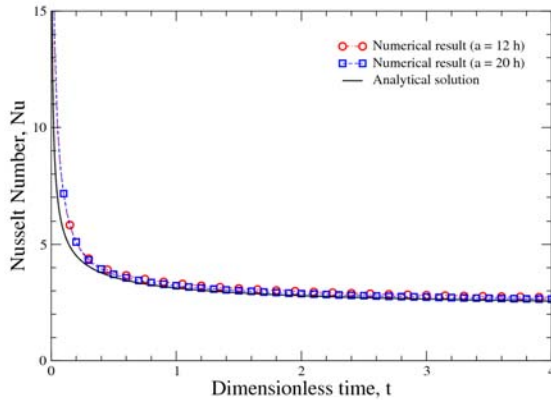


Figure 3: The evolution of overall Nusselt number of both analytical solution and numerical results.

We have also computed the temperature field around the sphere and compared it with analytical solution. Figure 4 shows the temperature contours at three different times. The right side of each image is the numerical solution of temperature contour at a center plane, while the left side is analytical solution from Equation (10). It is seen that at short time or in the inner region (close to the sphere), the numerical and analytical results matches very well. However, as time increases, the outer temperature starts to deviate the analytical solution because of the limitation of small computational domain size used in the present simulation.

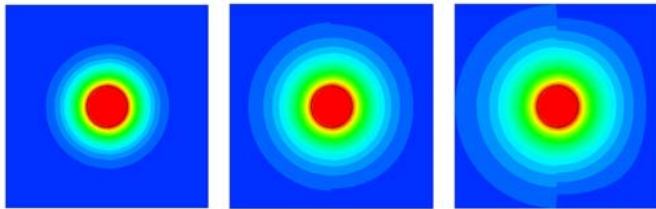


Figure 4: Temperature from both numerical and analytical solutions at $t=1, 3$ and 6 .

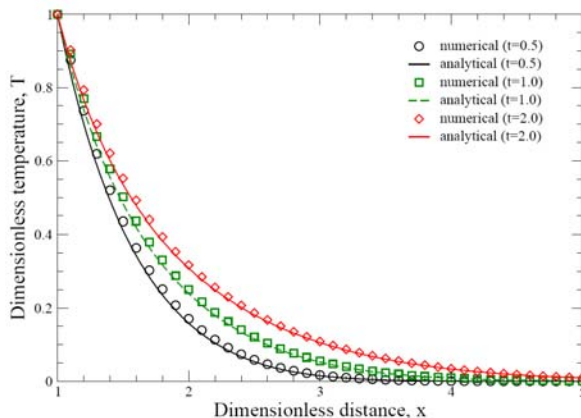


Figure 5: Temperature distribution around the sphere at $t=0.5, 1$ and 2 .

The quantitative results of temperature as a function of x (defined as the distance away from the center of sphere) are plotted in Figure 5. Excellent agreement is found between numerical results and analytical solutions for $t \leq 2$.

Our numerical results on unsteady conduction from a sphere show that the IB method can be effectively applied to enforce the constant temperature condition on particle boundary. Such approach can be easily extended to particle of complex geometry.

Falling of spheres of different temperature

When the temperature of a particle and its surrounding fluid is not the same, heat is transferred between particle and fluid. The heat flux influences the properties of the surrounding fluid and changes the dynamics of the sedimentation of the particle. We have examined the effects of the thermal interaction on the sedimentation velocity and the drag coefficient of a single circular particle settling in a fluid. [8] We found that at Grashof number $Gr=100$ the thermal interaction from the settling particle increases the hydrodynamic force on a hotter particle by a factor of two or it can reduce this force on a colder particle by more than 50% for Reynolds number Re around 20. This is a very significant result on the sedimentation of particles that maintain a temperature different than that of the fluid. In such cases, the sedimentation velocity of the particles depends strongly on the rate of thermal energy produced or consumed by the particle. At a very high Grashof number, a particle can even overcome the force of gravity and rise upward.

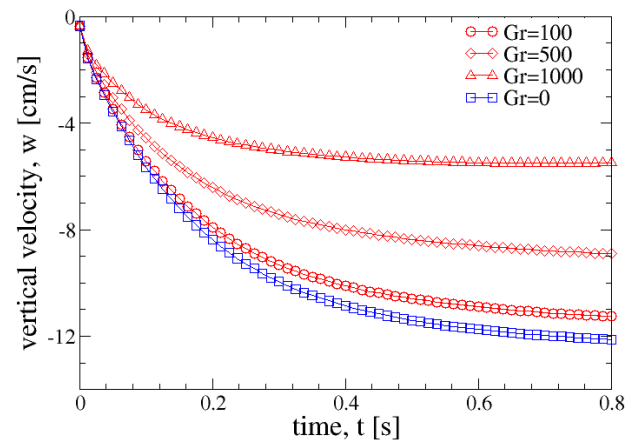


Figure 6: Settling velocity of a sphere at different Gr.

Here, we extend the DNS method to three-dimensional thermal interaction. As a preliminary study, we consider the sedimentation of spheres with different temperatures in a liquid column. The sphere has a radius of $a=0.75 \text{ cm}$ and density of $\rho_p=1.17 \text{ g cm}^{-3}$; the fluid has a density of $\rho_f=0.96 \text{ g cm}^{-3}$ and viscosity $\eta_f=0.58 \text{ P}$. The fluid Prandtl number is $Pr=0.7$. We investigate the effect of Grashof number to the particle sedimentation velocity.

Figure 6 shows the settling velocity of a sphere at four different Grashof numbers. It is seen that the velocity of hot particle of $Gr=1000$ is less than half compared to the case of a particle with the same temperature as fluid ($Gr=0$); this is because the large upward buoyancy force exerted on the particle at high Grashof number.

Figure 7 shows a snapshot of two spheres, one is of the same temperature with fluid, the other is of higher temperature, falling in an enclosure at $t=0.86$ s. The two spheres are initially positioned at the same level. The fluid velocity vector map on the vertical center plane is also shown. It is seen that the blue sphere ($Gr=0$) falls much faster than the red one ($Gr=1000$).

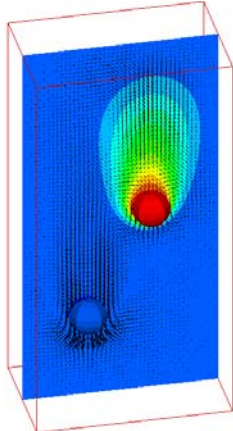


Figure 7: Snapshot of two spheres falling in a fluid at $t=0.86$ s for $Gr=1000$

REFERENCES

1. M. Ishii and T. Hibiki, "Thermo-fluid dynamic theory of two-phase flow," *Eyrolles*, (1975).
2. T. Tsuji, T. Tanaka, and T. Ishida, "Lagrangian numerical simulation of plug flow of cohesionless particles in a horizontal pipe," *Powder Technology* 71:239–250 (1992).
3. J. Feng, H. H. Hu, and D. D. Joseph, "Direct simulation of initial value problems for the motion of solid bodies in a Newtonian fluid Part 1. Sedimentation," *J. Fluid Mech.*, 261:95-134 (1994).
4. C. S. Peskin, "Numerical analysis of blood flow in the heart," *J. Comput. Phys.*, 25: 220–252 (1977).
5. J. Mohd-Yusof, "Combined immersed boundaries/B-splines methods for simulations of flows in complex geometries," *Annual Research Briefs*, Center for Turbulence Research, Stanford University (1997).

CONCLUSIONS

A numerical method that is based on DNS and solves both the momentum and heat interactions in particulate flows has been presented. In order to enforce the rigid body motion of solid particles, a force density function has been placed in the entire region where the particles are present. This force density field has been calculated using a direct-forcing scheme. We used an analogous method and an energy density function to enforce the uniform temperature conditions in the regions that are occupied by particles of high thermal conductivity. The velocity of the particles is obtained by solving the set of ordinary differential equations, which represent the Lagrangian equation of motion of the particles. The numerical method developed was validated by comparisons with the case of unsteady conduction of a sphere in a large domain. Results of the sedimentation of particles with different temperatures show how the local temperature field and buoyancy force affects the particle sedimentation process; it also shows that the IB based DNS method is capable to solve particulate flow problems where the particulate motion and heat transfer occur simultaneously.

ACKNOWLEDGEMENTS

This work is partly supported by a grant from the DOE, DE-NT0008064 to UTSA, Mr. Steven Steachman is the program manager.

6. Z.-G. Feng and E. E. Michaelides, "Proteus: A direct forcing method in the simulations of particulate flow," *J. Comput. Phys.*, 202: 20-51 (2005).
7. M. Uhlmann, "An immersed boundary method with direct forcing for the simulation of particulate flows," *J. Comput. Phys.*, 209: 448-476 (2005).
8. Z.-G. Feng and E. E. Michaelides, "Inclusion of Heat Transfer Computations for Particle Laden Flows," *Physics of Fluids*, 20:675-684 (2008).
9. Z.-G. Feng and E. E. Michaelides, "Heat transfer in particulate flows with direct numerical simulation (DNS)," *Int. J. Heat Mass Transfer*, 52:777-787 (2009)
10. Z.-G. Feng and E. E. Michaelides, "Heat transfer in particulate flows with direct numerical simulation (DNS)," *Int. J. Heat Mass Transfer*, 52:777-787 (2009).
11. Z-G Feng and E. E. Michaelides, "Unsteady heat transfer from a sphere at finite Peclet numbers," *ASME Journal of Fluids Engineering*, 118:96-102 (1996).